



Absolute cross sections from X - γ coincidence measurements

A. Lemasson^a, A. Shrivastava^b, A. Navin^a, M. Rejmund^a, V. Nanal^c, S. Bhattacharyya^d,
A. Chatterjee^b, S. Kailas^b, K. Mahata^b, V.V. Parkar^b, R.G. Pillay^c, K. Ramachandran^b,
P.C. Rout^b

^aGANIL, CEA/DSM - CNRS/IN2P3, Bd Henri Becquerel, BP 55027, F-14076 Caen Cedex 5, France

^bNuclear Physics Division, Bhabha Atomic Research Centre, Mumbai 400085, India

^cDept. of Nuclear and Atomic Physics, Tata Institute of Fundamental Research, Mumbai 400005, India

^dVariable Energy Cyclotron Centre, 1/AF Bidhan Nagar, Kolkata 700064, India.

Abstract

An activation technique using coincidences between characteristic X-rays and γ -rays to obtain absolute cross sections is described. This method is particularly useful in the case of nuclei that decay by electron capture. In addition to the reduction of possible contamination, an improved detection sensitivity is achieved as compared to inclusive measurements, thereby allowing the extraction of absolute fusion cross sections in the nano-barn range. Results of this technique for ${}^6\text{Li} + {}^{198}\text{Pt}$ system, at energies around the Coulomb barrier are described. Future applications with low intensity radioactive ion beams are also discussed.

Key words: X- γ coincidences, Activation, Fusion reactions, Absolute cross sections

1. Introduction

In general, it is necessary to reach the measurement limits to constrain the existence of new phenomena in any field of physics. The measurements of low cross sections for various nuclear processes similarly allow a detailed test of model assumptions. The recent evidence for a faster fall of the measured fusion cross section as compared to theoretical predictions at energies much lower than the Coulomb barrier and its astrophysical implications have been discussed in Ref. [1]. The availability of low intensity ($\sim 10^5$ pps) radioactive ion beams provides the opportunity to study the effect of exotic structures on the reaction mechanism. Both these studies require making sensitive measurements and employing techniques which are able to extract a weak signal in the presence of a relatively large background.

The fusion cross section is extracted from direct or indirect measurements of evaporation residues. The direct detection of evaporation residues can be performed using a recoil mass separator [1]. In the case of light and low incident energy beams, the small recoil energies and large charge of the residue make these measurements difficult. Measurements of in-

beam characteristic γ -decay of excited evaporation residues is another way of measuring the evaporation residues cross sections [2]. It is thus possible to measure the individual evaporation residue cross sections and hence the (sum) total fusion cross section. If the evaporation residues are unstable, the decay to the daughter nucleus can be measured. In cases where some of the evaporation residues are stable, corrections need to be made to obtain the total fusion cross section thus restricting the application of this technique.

Activation techniques when applicable, offer both a unique identification of the nucleus (obtained from the knowledge of the energy and half-life of the γ/α decay) and also a relatively lower background. In-beam and off-beam γ -ray spectroscopy methods [3] and measurements of α decay [4,5] have been used to obtain fusion cross sections. Moreover, if the evaporation residues are decaying by electron capture, the observation of delayed X-rays offers a further advantage. During the electron capture, an atomic electron is captured by the nucleus, leaving a hole in an atomic level. X-rays or Auger electrons will be emitted in the subsequent deexcitation of the atom. The description of this technique, its application and

limitations to obtain absolute fusion cross section have been discussed in Ref. [6]. These two off-beam techniques can be combined, using coincidences between the characteristic X-rays and γ -rays from the decay of an evaporation residue. The coincidences between X-rays and γ -rays increases the detection sensitivity by minimizing the background. Such a coincidence technique has been applied for nuclear spectroscopic studies of fission fragments to obtain an additional selectivity in building the relevant level schemes [7]. X - γ - ray coincidences were also used to obtain the average X-ray multiplicity and subsequently the evaporation residue cross section [8].

In the following sections, the application of the X- γ coincidence method to the ${}^6\text{Li} + {}^{198}\text{Pt}$ system at energies around the Coulomb barrier V_C (~ 30 MeV) is discussed. Results of this technique are compared with an inclusive measurement at $E_{lab} = 35$ MeV. The sensitivity of the method is exemplified from the measurements of low cross sections at energies well below the Coulomb barrier. The applicability of this method to measurements with low intensity radioactive ion beams is also discussed.

2. Description of the method

Evaporation residues, produced in the fusion of an energetic projectile bombarding a target, are stopped in the target and catcher assembly. After removal from the irradiation setup, the target+catcher (sample) is placed in an offline counting system. In the present case, the sample was placed in between two HpGe detectors and its activity was measured over a period of a few half-lives. If the evaporation residues are decaying by electron capture, the observation of delayed X-rays in coincidence with γ -ray decay characterize the nucleus of interest and lead to a reduction of the background. As the emission of X and γ -ray are independent processes, there are no angular correlation effects unlike in the case of γ - γ coincidences.

From simple principles of radioactive decay, the evaporation residue cross section can be obtained for a one step decay [3]:

$$\sigma_{ER} = \frac{N_c \lambda}{\varepsilon_\gamma f_\gamma \varepsilon_X f_X N_t I [1 - \exp(-\lambda \tau_{irr})] \times [\exp(-\lambda t_1) - \exp(-\lambda t_2)]^{-1}} \quad (1)$$

In the above equation (that can be generalized) N_c is the number of X- γ coincidences detected between times t_1 and t_2 after the irradiation of the sample, ε_γ (ε_X) the absolute photo peak efficiency for a given γ (X)-ray, f_γ (f_X) are the absolute intensities of the γ (X)-ray. λ is the radioactive decay constant of the evaporation residue, τ_{irr} is the irradiation

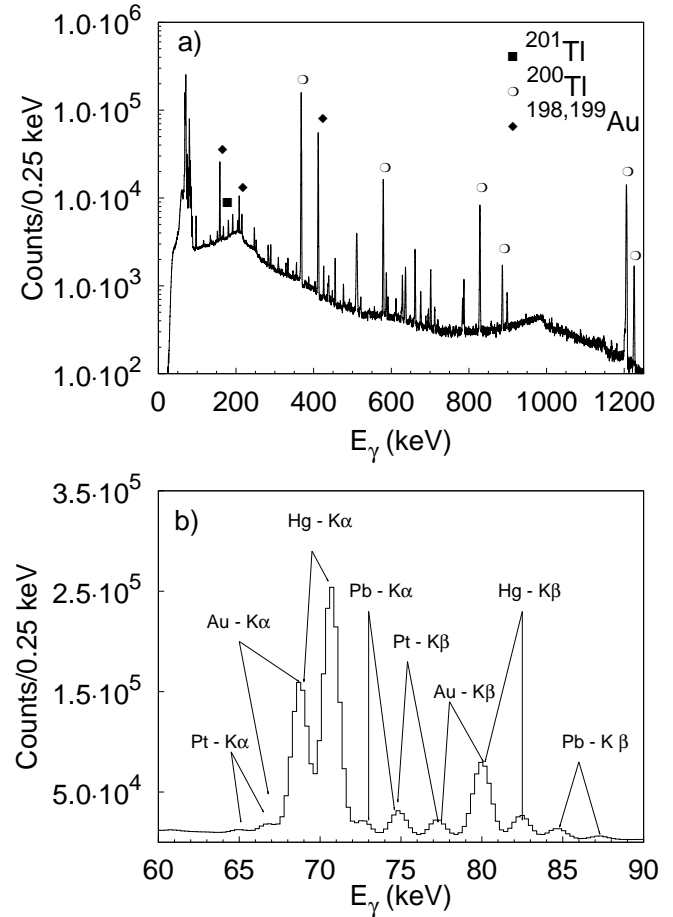


Fig. 1. a) Inclusive activation γ -ray spectra for the ${}^6\text{Li} + {}^{198}\text{Pt}$ system at E_{lab} of 35 MeV. Data were taken for 5.7 hours, 3.7 hours after a 3-hour irradiation. The dominant γ -rays arising from fusion and incomplete fusion reactions are labeled. b) An expanded view of the X-ray region shown in a).

time, N_t is the number of target atoms and I is the number of incident beam particles.

The coincidence yields are extracted by demanding an X-ray and obtaining the yield of the coincident γ -ray, or vice versa. It may be noted that the characteristic X-rays can also arise from internal conversion of the γ -rays in the daughter nucleus. In the next section, measurements at a few energies in the ${}^6\text{Li} + {}^{198}\text{Pt}$ system are presented to highlight various aspects of the method. The fusion excitation function measured over a wide energy range will be discussed elsewhere [9].

3. Experimental procedure and analysis

The measurements were carried out using beams of ${}^6\text{Li}$ provided by the BARC-TIFR 14UD Pelletron accelerator at Mumbai. These beams, with laboratory energies between 20 and 45 MeV, were used to irradiate 95.7% enriched ${}^{198}\text{Pt}$ targets having a typical thickness of ~ 1.3 mg/cm². A 2 cm \times 2 cm sheet

was weighed by a precision balance to determine the foil thickness before making four targets. The recoiling heavy residues were stopped in the target and an Al catcher foil ($\sim 1 \text{ mg/cm}^2$). The intensity of the beam during the irradiation, was typically between 5 to 25 pA and was monitored at one minute intervals. A commercially available current integrator was calibrated using a standard high precision current source. The uncertainty in the current measurement was less than 3%. The beam spot size was restricted to less than 3 mm diameter using a collimator close to the target. Following irradiations of duration varying from 3 to 54 hours, the target and catcher foil were placed in between two HpGe coaxial detectors, having Be windows, positioned 180° to each other. HpGe detectors had a diameter of $\sim 55 \text{ mm}$ and a length of $\sim 75 \text{ mm}$. The coincidence measurements were made in two geometries with detectors placed at opposite side of the sample : a) front faces of both the detectors at a distance of 10 cm from the sample b) in a close geometry where the front faces of both the detectors were at a distance of 1.5 mm from the sample. The minimum time between the end of the irradiation and the beginning of the counting was $\sim 10 \text{ min}$. The measurements were performed within a 10 cm thick Pb shield to reduce background from cosmogenic and natural radioactivity. Further the HpGe detectors were wrapped with thin sheets of Cu-Cd to cut down the Pb X-rays. The energy signals from both the detectors and the signal from a Time to Amplitude Converter between the detectors were recorded (1 μs range) on an event by event basis. The trigger to the acquisition system [10] was obtained from an OR condition of the constant fraction signals of the detectors. The electronic dead time was measured independently for each detector using a 10 Hz pulser and was found to be typically less than 1%.

The energy resolution of the HpGe detectors was $\sim 1 \text{ keV}$ at 80 keV, which allowed the separation of the $K_{\alpha 1}$ and $K_{\alpha 2}$ X-rays in the region of interest. The absolute efficiencies of the detectors were determined using a set of calibrated radioactive sources (^{57}Co , ^{133}Ba , ^{152}Eu and ^{241}Am) mounted in the same geometry and absorption conditions as the target. The overall error in the absolute efficiency was estimated to be less than 5%. In order to increase the detection efficiency for measurements at lower beam energies, the sample was placed between the two detectors in a close geometry (1.5 mm from each detector face). Coincidence summing effects, corresponding to the simultaneous detection of two or more γ -rays in a detector, have to be taken into account to obtain the cross sections in such a geometry [11, 12]. These effects were verified to be negligible at 10 cm. These corrections are only dependent on the decay scheme of the relevant nuclei. In the present case due to simplicity of the decay schemes of the nuclei, the correc-

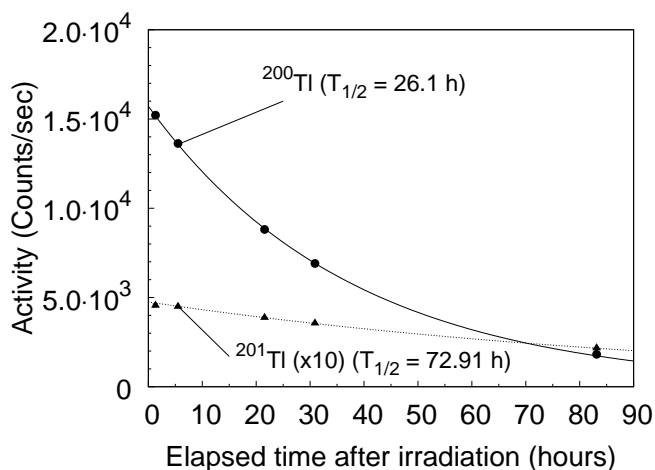


Fig. 2. Activity as a function of the elapsed time after irradiation for the 367.9 keV (^{200}Tl) and 167.5 keV (^{201}Tl) transitions at $E_{lab} = 35 \text{ MeV}$. The full and dotted lines are the fitted activities incorporating the known half-life of the ^{200}Tl and ^{201}Tl evaporation residues respectively.

tion could be easily accounted for. The nucleus dependent correction factor was determined from the measurements in both the geometries at three different beam energies.

The compound nucleus, ^{204}Tl , decays predominantly to the $^{199-202}\text{Tl}$ isotopes by neutron evaporation at the energies studied here. These evaporation residues are unstable and decay by electron capture to $^{199-202}\text{Hg}$ respectively. Additionally, due to the weak binding of the projectile (1.45 MeV), large cross sections for residues arising from breakup-fusion and/or transfer reactions were also observed. Some of these Tl isotopes have medical applications, hence their half-lives and the branching ratios for γ -emission from the daughter nuclei have been measured recently to a large accuracy [13, 14]. Figure 1a shows a typical inclusive γ -ray spectrum measured at $E_{lab} = 35 \text{ MeV}$. The relevant γ -rays corresponding to the decay of the Tl, Au and Pt isotopes arising from fusion, incomplete fusion and neutron transfer are identified. In addition to their energy, the origin of the γ -rays was also identified from the measurement of their half-lives. The measured γ -ray activities for the ^{200}Tl (26.1 (1) h) and ^{201}Tl (72.91 (4) h) evaporation residues as a function of time at 35 MeV are shown in Fig. 2. As can be seen from the figure, the data are consistent with the known half lives.

A typical $\gamma - \gamma$ coincidence matrix measured at $E_{lab} = 25 \text{ MeV}$ (an energy lower than the Coulomb barrier) is shown in Fig. 3. The back to back geometry of the detectors maximizes the collection of nearly backscattered events where a γ -ray deposits part of its energy in one detector and then scatters to the other detector. These events correspond to the diagonal lines, in the figure, having fixed energies such that $E_\gamma = E_{\gamma 1} + E_{\gamma 2}$. The γ -rays in coincidence with

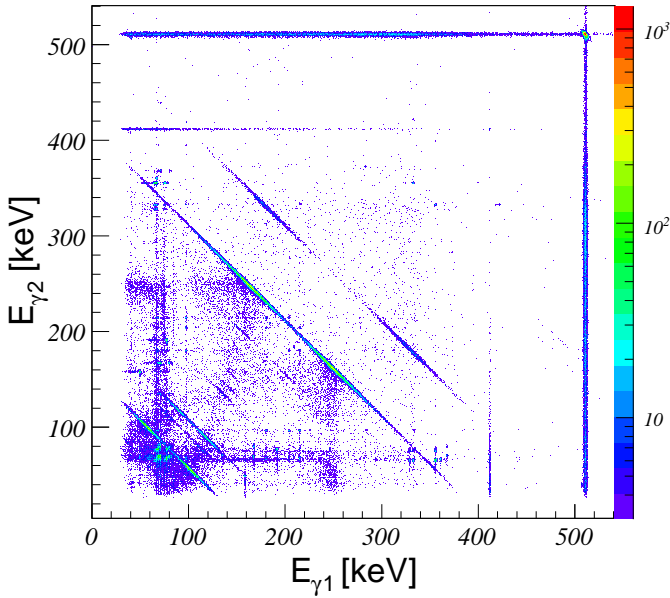


Fig. 3. (color online) A part of the two dimensional coincidence matrix at $E_{lab} = 25$ MeV with the sample at 1.5 mm from the face of the detectors. The data correspond to an irradiation of 14 hours and counted for 12 hours, 136 hours after the end of the irradiation.

X-rays can be clearly seen. A projection of such a coincidence matrix is used to obtain the relevant spectra to extract the cross sections. Figure 4 shows both the X-ray and γ -ray coincident spectra at $E_{lab} = 35$ MeV where the measured coincident yields are large. Figure 4a shows the X-rays that are in prompt coincidence with the 367.9 keV γ -ray in ^{200}Hg . Characteristics $K_{\alpha 1,2}$ and $K_{\beta 1,2}$ Hg X-rays arising from the electron capture can be seen. It should be noted that the contamination of the $K_{\alpha 2}$ Hg X-ray with $K_{\alpha 1}$ Au X-ray shown in Fig 1b, is removed as a consequence of the γ -coincidence condition. A comparison between the coincidence (Fig. 4) and the related inclusive (Fig. 1) γ -ray spectra shows that the coincidence condition removes the uncorrelated transitions leading to a substantial reduction of the level of the background. For example, the peak to background ratio for the 367.9 keV γ -ray was found to be around two orders of magnitude larger in the coincidence spectrum than in the inclusive one. The X- γ -ray coincidence yields can be extracted from the four X-ray yields ($K_{\alpha 1}$, $K_{\alpha 2}$, $K_{\beta 1}$ and $K_{\beta 2}$) shown in Fig. 4a. Their well determined intensity ratios act as a consistency check of these yields. The X- γ -ray coincidence yields can also be extracted from γ -ray yields obtained by gating on the Hg X-rays (Fig. 4b). The relevant γ -rays corresponding to the decay of the evaporation residues ($^{199,200,201}\text{Tl}$) can be seen. The $^{198,199}\text{Tl}$ residue can also arise from interactions with ^{196}Pt (2.56% impurity) in the target. The corrections for these channels are suitably taken into account to obtain the total fusion cross sections. In the remaining

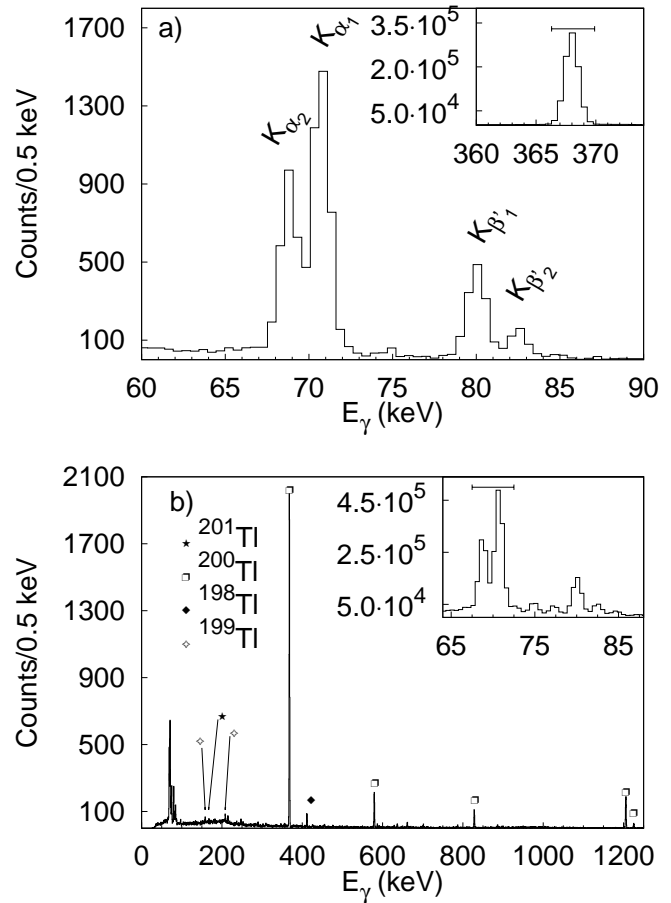


Fig. 4. a) X-ray spectrum in coincidence with the 367.9 keV γ -ray transition (corresponding to the decay of ^{200}Tl) at $E_{lab} = 35$ MeV. The inset shows the γ -ray coincidence condition. b) γ -ray spectrum in coincidence with K_{α} X-rays of Hg at $E_{lab} = 35$ MeV and the X-ray coincidence condition (inset). These exclusive spectra are to be compared with the inclusive measurements shown in Fig. 1.

part of the paper the cross sections have been predominantly obtained using the method illustrated in Fig. 4b. A similar analysis was performed at other energies.

4. Results and Discussion

The evaporation residue cross sections extracted using both inclusive γ and X- γ exclusive measurements for the $^6\text{Li} + ^{198}\text{Pt}$ system at 35 MeV are compared in Table 1. Residue cross sections were extracted using Eq. 1 and absolute γ and X-rays intensities were taken from [13,14]. The errors were estimated from the variance-covariance matrix, considering the peak height and background parameters as variables [10]. As can be seen from the Table 1 there is a good agreement between inclusive and coincidence methods showing the reliability of the present technique to obtain the cross section.

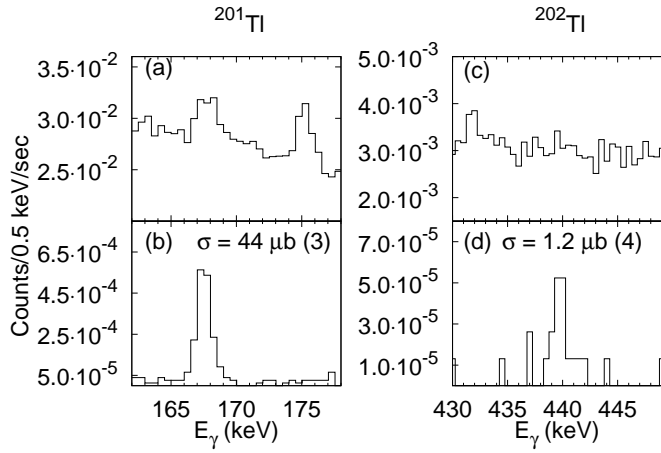


Fig. 5. γ -ray spectra at $E_{lab} = 23.6$ MeV. Expansion of the relevant regions of interest corresponding to the evaporation residue ^{201}Tl and ^{202}Tl , characterized by the 167.5 keV and 439.6 keV transitions respectively. (a) and (c) are the inclusive spectra and (b) and (d) correspond to $X(K_{\alpha})$ - γ coincidence spectra.

Table 1

Evaporation residue cross sections for $^{200,201}\text{Tl}$ at $E_{lab} = 35$ MeV obtained using different detector to sample distances (see text).

	Inclusive (10 cm)	Coincidence (10 cm)	Coincidence (1.5 mm)
Channel	(mb)	(mb)	(mb)
^{201}Tl	25.7 (0.9)	-	24.8 (1.1)
^{200}Tl	308 (2)	314 (8)	309 (2)

The non-observation of the ^{201}Tl residue is consistent with the low coincidence efficiency for a detector to sample distance of 10 cm.

The sensitivity of the measurements to obtain low cross sections at energies well below the barrier are discussed below. Figure 5 shows the region of interest of the inclusive and coincident γ -spectra (gated by the K_{α} X-ray of Hg) for the $^{201,202}\text{Tl}$ nuclei. Figure 5a shows that the 167.5 keV γ -ray (^{201}Hg) is riding on a large background, arising from Compton events of higher energy γ -rays. It can be seen from the coincidence spectrum shown in Fig. 5b, that the background level is drastically reduced, leading to a peak to background ratio ~ 70 times larger than in the case of the inclusive spectrum. Such an improvement leads to a more accurate and reliable determination of the γ yields, necessary to obtain the fusion cross section. Figs. 5 c-d re-emphasize this for the 439.6 keV γ -ray (^{202}Hg) where a much smaller cross section is involved. In the inclusive γ -ray spectrum (Fig. 5c), the yield of the 439.6 keV γ -ray is not visible over the background. On the contrary, the 439.6 keV γ -ray can be clearly observed in the coincidence spectrum (Fig. 5d). The extracted evaporation residue cross-sections for the two channels are also indicated in figures 5 and 6.

Figure 6 shows the γ -ray spectra measured at

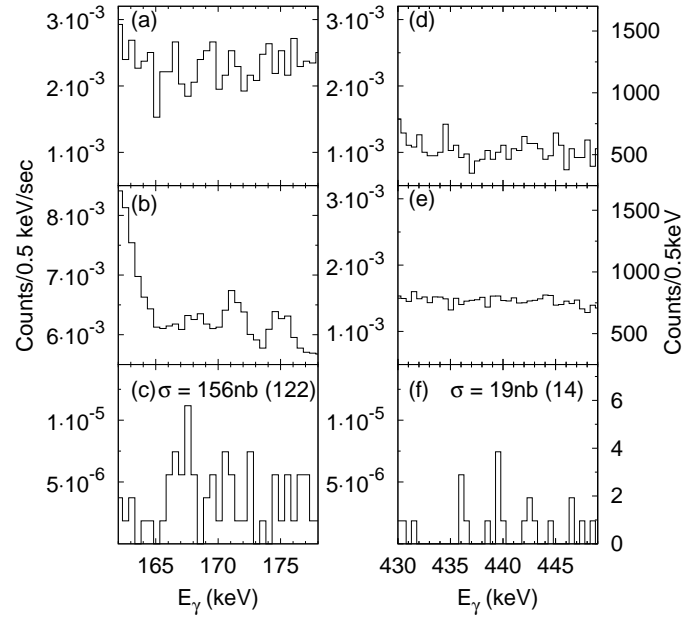


Fig. 6. γ -ray spectra at $E_{lab} = 20.6$ MeV. Expansion of the relevant regions of interest corresponding to the evaporation residue ^{201}Tl and ^{202}Tl , characterized by the 167.5 keV and 439.6 keV transitions respectively. (a) and (d) correspond to the background spectra collected without a sample. (b) and (e) correspond to the inclusive spectra, (c) and (f) correspond to the X - γ coincidence spectra.

20.6 MeV corresponding to the data at the lowest measured energy ($E/V_B \sim 0.66$). The data shown was collected for 54 hours after an irradiation of 56 hours. At this energy the comparison between the inclusive (Figs. 6b and 6e) and coincidence (Figs. 6c and 6f) spectra clearly shows the significant increase of detection sensitivity resulting from the present coincidence technique. Poisson statistics and the maximum likelihood method [15] using CERN software package ROOT were used to obtain the quoted errors. This measurement of the absolute cross section down to the nanobarn level is a significant achievement.

In the remaining part of this section, limits arising from background on the extracted cross section are discussed. A comparison between the background spectra collected without a sample (Figs. 6a and 6d) and inclusive spectra (Figs. 6b and 6e) shows that the lower limit of the sensitivity of the measurement is presently not limited by the room background. The cross sections for $^{198,199}\text{Au}$ arising from d capture is measured to be ~ 4 orders of magnitude larger. The Compton scattered γ -rays from their daughter nuclei ($^{198,199}\text{Hg}$) thus contribute to background in the X-rays region. In addition to the above, in the case of the 439.6 keV + 70.8 keV X- γ coincident events, the Compton scattered events from the 511 keV γ -rays lead to a larger background level in the region of

interest. This can be seen from the two dimensional spectra shown in Fig. 3 where the intersection of the diagonal line ($E_\gamma = E_{\gamma 1} + E_{\gamma 2} = 511$ keV) and the gating X-ray transition is overlapping with the γ -ray of interest limiting the measured peak to background. Thus the sensitivity of the present measurement can be further improved by minimizing products formed in unwanted reactions leading to the emission of 511 keV γ -rays.

5. Applications to Radioactive Ion Beams

As described above, the lowest cross sections measured was a few nb with a typical beam intensity of 10^{11} pps. Using the delayed X-rays method measurements with ${}^6\text{He} + {}^{64}\text{Zn}$ (10^6 pps) the authors of [16] were able to measure a total cross section as low as 50 mb. The application of the delayed X-rays technique for the extraction of the fusion cross sections in the case of high Z evaporation residues is relatively more difficult due to the dominance of neutron evaporation channels (thus characterized by the same X-rays). Using off beam α decay measurements, Penionzhkevich *et al.* [5] were able to measure cross sections of 1 mb for the ${}^6\text{He}+{}^{206}\text{Pb}$ system.

GANIL is presently the only facility in the world to deliver low energy beams of the doubly Borromean nucleus ${}^8\text{He}$. The only fusion cross section measurements with ${}^8\text{He}$ beams were performed using the inclusive in-beam γ -ray technique [17]. It was not possible to measure low cross sections at energies below the Coulomb barrier due to the competition with room background. With the technique and improved sensitivity discussed in this article it will be possible to measure sub-barrier fusion cross sections with a weakly bound ${}^8\text{He}$ beam and address the fundamental questions of multidimensional tunneling including coupling to the continuum.

6. Conclusion

The agreement between the inclusive and coincidence methods shows that the X- γ coincidence method suggested here can be reliably applied to obtain absolute cross section. This technique thus leads to a greater precision and accuracy of the measured cross sections down to the nanobarn level and is ideally suited for measurements with low intensity radioactive ion beams.

7. Acknowledgments

We would like to thank P. Patale and M.S. Pose for their help during the experiment and the Pelletron group for a smooth operation. We also thank Y. Blumenfeld for providing the ${}^{198}\text{Pt}$ targets. One of

us (A.L.) was partly supported by the Region Basse-Normandie (France).

References

- [1] C. L. Jiang, K. E. Rehm, H. Esbensen, R. V. F. Janssens, B. B. Back, C. N. Davids, J. P. Greene, D. J. Henderson, C. J. Lister, R. C. Pardo, T. Pennington, D. Peterson, D. Seweryniak, B. Shumard, S. Sinha, X. D. Tang, I. Tanihata, S. Zhu, P. Collon, S. Kurtz, and M. Paul, *Phys. Rev. C* 71, (2005) 044613.
- [2] A. Navin, V. Tripathi, Y. Blumenfeld, V. Nanal, C. Simenel, J. M. Casandjian, G. de France, R. Raabe, D. Bazin, A. Chatterjee, M. Dasgupta, S. Kailas, R. C. Lemmon, K. Mahata, R. G. Pillay, E. C. Pollacco, K. Ramachandran, M. Rejmund, A. Shrivastava, J. L. Sida, and E. Trygggestad, *Phys. Rev. C* 70, (2004) 044601.
- [3] P. R. S. Gomes, T. J. P. Penna, R. Liguori Neto, J. C. Acquadro, C. Tenreiro, P. A. B. Freitas, E. Crema, N. Carlin Filho and, M. M. Coimbra, *Nucl. Instr. and Meth. A* 280 (1989) 395.
- [4] M. Dasgupta, D. J. Hinde, R. D. Butt, R. M. Anjos, A. C. Berriman, N. Carlin, P. R. S. Gomes, C. R. Morton, J. O. Newton, A. Szanto de Toledo, and K. Hagino *Phys. Rev. Lett.* 82, 1395 (1999)
- [5] Yu. E. Penionzhkevich, V. I. Zagrebaev, S. M. Lukyanov, and R. Kalpakchieva, *Phys. Rev. Lett.* 96, 162701 (2006).
- [6] R.G. Stokstad, Y Eisen, S. Kaplanis, D. Pelte, U Smilansky and I. Tserruya, *Phys. Rev. C* 21 (1980) 2427.
- [7] K. Butler-Moore, R. Aryaeinejad, J.D. Cole, Y. Dardenne, R.C. Greenwod, H.M. Winston, *Nucl. Instr. and Meth. A* 361 (1995) 245.
- [8] H. J. Karwowski, S. E. Vigdor, W. W. Jacobs, S. Kailas, P. P. Singh, F. Soga, T. G. Throwe, T. E. Ward, D.L. Wark, J. Wiggins, *Phys. Rev. C* 25 (1982) 1355.
- [9] A. Shrivastava *et al.*, (to be published).
- [10] Data Acquisition and Analysis Package LAMPS. (<http://www.tifr.res.in/~pell/lamps.html>)
- [11] K. Debertin and U. Schotzig, *Nucl. Instr. and Meth.* 158 (1979) 471.
- [12] K. Debertin, R. G. Helmer, *Gamma- and X-ray Spectrometry with Semiconductor Detectors*. Elsevier Science Publishers, Amsterdam, The Netherlands (1988)
- [13] Nucleide, Nuclear and Atomic Decay Data (2005), (http://www.nucleide.org/DDEP_WG/DDEPdata.htm); Evaluated Nuclear Structure Data File (ENSDF) : (<http://www.nndc.bnl.gov/ensdf/>)
- [14] Karla C. de Souza, Mnica L. da Silva, Jos U. Delgado, Roberto Poledna, Ricardo T. Lopes, Carlos J. da Silva, *Appl. Radiat. Isot* 60 (2004) 307.
- [15] W.-M. Yao *et al.*, *J. Phys. G* 33 (2006) 1.
- [16] A. Di Pietro, P. Figuera, F. Amorini, C. Angulo, G. Cardella, S. Cherubini, T. Davinson, D. Leanza, J. Lu, H. Mahmud, M. Milin, A. Musumarra, A. Ninane, M. Papa, M. G. Pellegriti, R. Raabe, F. Rizzo, C. Ruiz, A. C. Shotter, N. Soic, S. Tudisco, and L. Weissman, *Phys. Rev. C* 69, 044613 (2004).
- [17] A. Lemasson *et al.*, (to be published).